Phase Shifts Induced by the Piezoelectric Transducers Attached to a Linearly Chirped Fiber Bragg Grating

Xuxing Chen, Yves Painchaud, Kazuhiko Ogusu, *Member, IEEE, OSA*, and Hongpu Li, *Member, IEEE, OSA*

***Abstract*—A simple method enabling to generate a stable and controllable phase shift in a linearly chirped fiber Bragg grating (FBG) is theoretically and experimentally demonstrated, which is based on the utilization of the mini-size piezoelectric transducers (PZTs). The magnitude of the induced phase shift can easily be controlled by adjusting the voltage applied on the individual PZT. With this method, a narrow bandpass filter with 3-dB band width of 0.085 nm is obtained. Based on this kind of filter, an Erbium-doped fiber ring laser is also demonstrated, and both switchable and stable single-longitudinal-mode (SLM) laser emission is successfully realized.**

***Index Terms*—Fiber Bragg gratings, lasers, phase shift, single-mode.**

I. Introduction

ATTRIBUTED to the inherent property of wavelength filtering with an ultra-narrow bandwidth, phase shifted fiber Bragg grating (FBG) has been widely used in the fields such as the fiber lasers [1]–[3], wavelength demultiplexing [4], fiber sensors [5], [6], and all optical logic devices [7], [8] etc. In general, a phase shift can be permanently inscribed into a FBG by using the phase shift phase-mask technique [9], [10], the UV post-processing [11], or the post-etching technique [12]–[14]. However, all of the above approaches need either an expensive phase mask or a very complicated control system for the grating's fabrication. Moreover, all of them are lack of the flexibility for the implementation of both tunable and switchable devices once the phase shift is inscribed in a FBG. On the other hand, a temporary phase shift can be introduced into a FBG by the thermal method [15]–[21], where a narrow NiCr wire is utilized to heat the local region of a FBG. Because of the thermal-expansion and thermal-optical effects, the refractive index of the local grating would change with the temperature. A phase shift will thus be introduced at the local point of the grating. The wavelength tunability of the resulted notch filter has been realized by moving the NiCr wires along the grating direction [18]. A comb filter can also be realized by utilizing either one wire in a sampled grating [3], [19] or multiple wires in a single channel FBG. However, the thermal method needs a high temperature to attain the stable π phase shift, which is hard to control in practice. Moreover, the temperature gradient and the expansion of the NiCr wire may make the phase shift not stable especially when the multiple wires are closely placed in order to generate multiple phase shifts in the FBG.

Besides the thermal method, the mechanical stretch method can also be imposed to introduce a temporary phase shift in a linearly chirped FBG (LCFBG). The pioneer work for the later one was firstly reported by Xu *et al.* in [22], where either a single or multiple phase shifts in a LCFBG were successfully demonstrated by using a piezoelectric stack. However, the detailed numerical analysis and dependence of the notch bandwidth on the phase shift had not been given. Moreover, the split-notch effect due to the birefringence of the FBG has not been investigated yet.

In this paper, the PZT-induced both switchable and stable phase shift in a linearly chirped FBG is theoretical and experimental demonstrated. The dual notches phenomenon due to the birefringence of the grating and the asymmetric stretching of the PZT is solved by utilizing a polarizer and a polarization controller. The magnitude of the induced phase shift can easily be changed by controlling the voltage imposed on the PZT. The wavelength tunability and the formation of the double notch filter in a chirped FBG have also been investigated when two PZTs are bonded to the grating simultaneously. Moreover, as an important application of this kind of phase-shift FBG to the Erbium-doped fiber (EDF) ring laser, both switchable and stable single-longitudinal-mode (SLM) laser emission [23]–[29] is successfully demonstrated.

II. PZT-Induced Phase Shift in a Linearly Chirped FBG

A. Principle of the Phase Shift in FBG

FBGs are fabricated by exposing an optical fiber to spatially varying pattern of ultraviolet intensity. In general, the induced refractive index-modulation Δn of a FBG can be expressed as

$$\Delta n(z) = \mathrm{Re}\left\{\left(\frac{\Delta n_1(z)}{2}\exp\left(i\frac{2\pi z}{\Lambda} + i\varphi_g(z)\right)\right)\right\} \quad (1)$$

where z is the position along the grating, Δn_1 is the maximum index-modulation, Λ is the central pitch of the FBG, φ_g is the local phase of the grating. Once the phase shifts θ_j $(j = 1, 2, \ldots, N)$ are introduced at the positions of z_j in the grating, the index modulation Δn_p can be expressed as [30]

$$\Delta n_p = \mathrm{Re}\left\{\frac{\Delta n_1(z)}{2}\cdot\exp\left(i\frac{2\pi z}{\Lambda} + i\varphi_g(z) + i\sum_j^N \theta_j \cdot q(z - z_j)\right)\right\} \quad (2)$$

Manuscript received March 03, 2010; revised May 09, 2010, May 18, 2010; accepted May 18, 2010. Date of publication June 01, 2010; date of current version July 05, 2010. This work was supported in part by the Grant-in-Aid for Scientific Research from JSPS in Japan, in part by the International Communications Foundation, and in part by the Hamamatsu Science and Technology Promotion in Japan.

X. Chen, K. Ogusu, and H. Li are with the Department of Electrical and Electronic Engineering, Shizuoka University, Johoku 3-5-1, Hamamatsu 432-8561, Japan (e-mail: dhli@ipc.shizuoka.ac.jp).

Y. Painchaud is with TeraXion Inc., Quebec, QC G1P4S8, Canada.

Color versions of one or more of the figures in this paper are available online at http://ieeexplore.ieee.org.

Digital Object Identifier 10.1109/JLT.2010.2051215

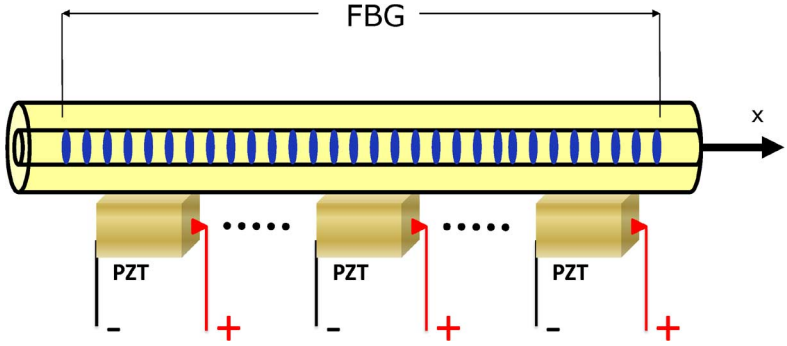

Fig. 1. Schematic diagram for the phase shifts induced by the PZTs in a FBG.

where N is the number of the inserted phase shifts and the function q is defined as: $q(z-z_j)=0$ if $z<z_j$ and $q(z-z_j)=1$ if $z\geq z_j$. Once all the parameters shown in (2) are known, the reflection spectrum for the phase-shift FBG can be easily obtained by using the well-known Transfer Matrix Method [31].

B. The PZT-Induced Phase Shift

Principle of the proposed approach is schematically shown in Fig. 1, where the PZTs provided by the Nihon Ceramic with a size of $3\times3\times3$ mm^3 and the maximum extension-region of 1 μm are wholly glued to the FBG along the grating direction. When the voltage is applied on the PZT, it will be extended. The accumulated phase change of the grating is then obtained at end point of the PZT and the phase shift θ introduced can be approximately expressed as

$$\theta \approx \frac{2\pi n_{\text{eff}}}{\lambda}\cdot\Delta L \tag{3}$$

where n_{eff} is the effective refractive index of the fiber, λ is the local Bragg wavelength where the PZT is located, and ΔL is the total length-change of the grating induced by the PZT. Unlike the one using the previous method [3], [19], there is no influence of the temperature gradient and the thermal expansion existed in the FBG. Therefore, multiple PZTs can be placed as close as possible to introduce multiple phase shifts in a FBG as shown in Fig. 1. The separation of these PZTs is only decided by the dimension of the PZT. Moreover, tunability for the phase shift can easily be realized by adjusting the voltage applied on the PZT itself.

C. Numerical Results for the Phase Shifted FBG

Here the layer peeling method [32]–[34] is used to design the grating structure. The grating is designed to have a length of 12 cm, a central wavelength λ_0 (=1538 nm) and a flat-top bandwidth $\Delta\lambda\sim10$ nm. The average effective refractive index of the grating is assumed to be 1.5, which corresponds to a center grating pitch of 0.513 μm. The target reflectivity is adopted as

$$r(\lambda)=\sqrt{0.9}\exp\left\{-(\ln 2)\left[\frac{\lambda-\lambda_0}{0.5\times\Delta\lambda}\right]^{12}\right\}\exp\{-i\Phi(\lambda)\} \tag{4}$$

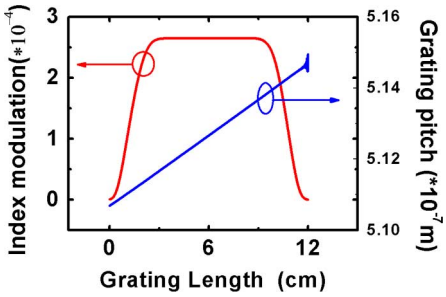

Fig. 2. Grating structure obtained by the layer peeling method with the parameters described in the text.

where $\Phi(\lambda)$ is the grating phase, which can be expressed by [33], [34]

$$\Phi(\lambda)=-c\int_{\lambda_{\min}}^{\lambda}(2\pi/x^2)D_2(x-\lambda_0)\mathrm{d}x \tag{5}$$

where c is the light velocity in the vacuum, $\lambda_{\min}$ is the start wavelength in the simulation, and D_2 is the chromatic dispersion. In our case, the range of the wavelength considered is 50 nm and the dispersion is -100 ps/nm. The obtained grating structures are shown in Fig. 2, where the refractive index-modulation profile and grating pitch versus the position are obviously shown. The maximum refractive index-modulation is about 2.65×10^{-4}. Once the grating structure is known, the different phase shifts can be inserted at different positions by changing the complex coupling coefficient according to (2). Then the Transform Matrix Method can be imposed to calculate the reflection spectrum for the phase-shift FBG, In our simulation, the grating is divided into multiple uniform sections with a step of 39 μm. Fig. 3 shows the reflection spectrum when seven different phase-shifts ranged from 0 to π are inserted at the center of the grating, respectively. The inset shows the details of the resulted spectrum. Note that only the phase shift rather than the real blank region (corresponding to the phase shift) of the grating is considered in our simulation. As a result, it can be seen that there really exists a stop-band (notch) at the center of the reflection spectrum when phase shift is inserted. The notch-depth increases as the magnitude of the inserted phase is gradually increased and reaches the maximum only when π

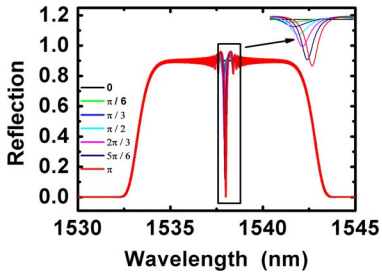

Fig. 3. Simulation results of the notch filter with different phase shift.

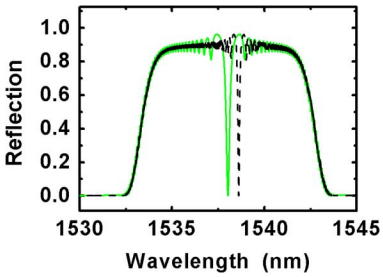

Fig. 4. Tunability of the notch filter with a wavelength shift of about 0.5 nm when a π phase shift is inserted at a different position. Solid line: the π phase shift inserted at the center of the grating. Dashed line: the π phase shift inserted on the right side of the center with a separation of 0.6 cm.

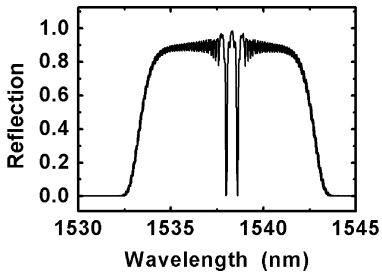

Fig. 5. Simulation results of the double notch filters with a wavelength spacing of about 0.5 nm when two π phase shifts are simultaneously inserted in the grating with a separation of 0.6 cm.

phase shift is inserted. Meanwhile, the bandwidth of the notch decreases with the increase of the phase shift.

Next we have investigated the wavelength tunability for the resulted notch filter. Fig. 4 shows the reflection spectrum when a π phase shift is inserted at two different positions respectively, where the solid line shows the π phase shift inserted in the center of the grating and the dashed line shows the π phase shift inserted on the right side of the center with a separation of 0.6 cm along the grating direction. It is seen that the notch wavelength can be tuned with a step of about 0.5 nm. With the same method, it is expected that the multiple-notch filter can be formed by simultaneously inserting multiple phase shifts into the grating. Fig. 5 shows a typical result for the reflection spectrum where two π phase shifts are simultaneously inserted into the grating. The spacing between the inserted positions of two phase-shifts along the grating is also assumed to be 0.6 cm. It is seen that nearly identical two notch filters with a wavelength separation of about 0.5 nm are produced just like what we expect.

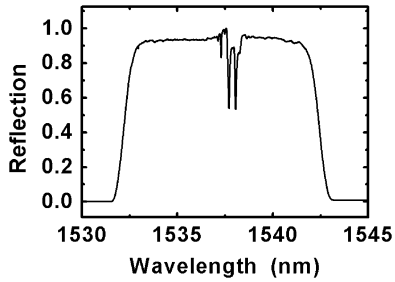

Fig. 6. Double notch filters appeared in the reflection spectrum, which happens due to the resident and the induced birefringence of the grating.

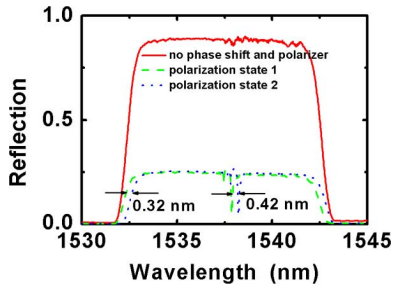

Fig. 7. Reflection spectrum with different polarization states. Solid line shows the case without phase shift and polarizer. Dashed line and dot line show the reflection with different polarization state when a π phase shift is inserted in the grating.

D. Experimental Results and Discussions

To confirm the above theoretical results, we perform several tests for a linearly chirped FBG (provided by TeraXion Inc.) with the phase shift introduced by applying the voltage on a PZT. The grating strength is about 10 dB with a length of about 12 cm and the flat-top bandwidth is about 10 nm, characteristics of which are nearly the same as the theoretical ones given above. Firstly, only one PZT is glued at the center of the grating and the applied voltage is 150 V. The reflection spectrum measured by using an optical spectrum analyzer (OSA) is shown in Fig. 6.

Unlike the theoretical one shown in Fig. 3, double notch filters rather the one appear in the reflection spectrum and their depths become small no more than 3 dB. We believe that this phenomenon is due to resident birefringence of the grating and the induced birefringence due to the asymmetric stretching of the PZT. This birefringence effect is not perceived without the phase shift inserted and becomes obvious when the phase shift is inserted. Each of the dips corresponds to the different polarization state. To verify the above thoughts, we add a polarizer and a polarization controller (PC) between the broadband light source and the FBG. Fig. 7 shows the results, where the solid line shows the reflection of the grating when the phase shift is not inserted and meanwhile the polarizer is not used. Dashed line and dot line show the reflection spectra with different polarization states when a phase shift is inserted into the grating. It is seen that the depth of the notch obtained when the polarizer and the PC are utilized is larger than the one without using the polarizer and reaches about 7 dB. The shift of the dips is about 0.42 nm and meanwhile the shift of the band edge is about 0.32 nm. The difference of the shift (0.1 nm) indicates that besides the original birefringence of the grating, the PZT-induced extension on the one side of the grating would introduce some

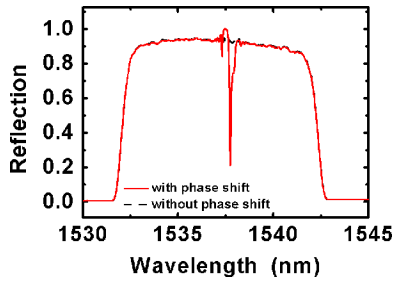

Fig. 8. Reflection spectrum of the linearly chirped FBG with one phase shift induced by a PZT (solid line) and the recovered reflection one when the voltage is removed (dashed line) after a polarizer and a PC are inserted.

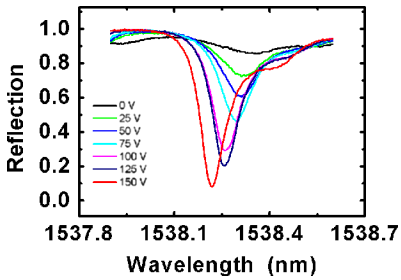

Fig. 9. Spectra of the notch filter at conditions of the different voltages applied on the PZT.

birefringence also. Therefore, in order to generate one dip with a narrower bandwidth, only one polarization state is selected in our experiment by carefully adjusting the PC. Fig. 8 shows the reflection spectrum (solid line) while the applied voltage is 150 V. It is seen that a single notch filter appears in the reflection band. The notch depth is about 7.5 dB and the 3-dB bandwidth of the induced notch is about 0.085 nm which may become narrower when the grating strength is increased further. The small peak appeared at the short wavelength side may be due to the asymmetric stretching of the grating. Because only one side of the grating is extended by the PZT, coupling of the core mode into a cladding mode may cause a loss in the reflection. When the applied voltage is removed, the reflection will recover to the original one as is shown in Fig. 8 (dashed line), which means that the resulted notch filter is switchable also. Profile of the notch (related to the induced phases) can also be changed by varying the applied voltages. Fig. 9 shows the notch spectrum at different voltages. It can be seen that the depth of the notch increases in accordance with the increment of the applied voltage, which agrees well with the simulation results shown in Fig. 3. However, the resonant wavelength has a blue shift, which indicates that there exists a decrease for the effective index of the local grating once the grating is lengthened, which is oppose to the previous one induced by the thermal effect [19]. When the voltage is further increased, the depth of the notch will decrease and the sidelobes appeared at the right hand of the notch will become more obvious, which can also be regard as a loss due to the coupling of the core mode to cladding mode. The stability for the induced notch is also investigated. Five measurements of the reflection spectrum are performed every other five minute by using an OSA. Fig. 10 illustrates the near view of the created notch in 1-nm range through the five scans when the voltage is fixed to 150 V. No wavelength and reflection shift can be seen in such a short range.

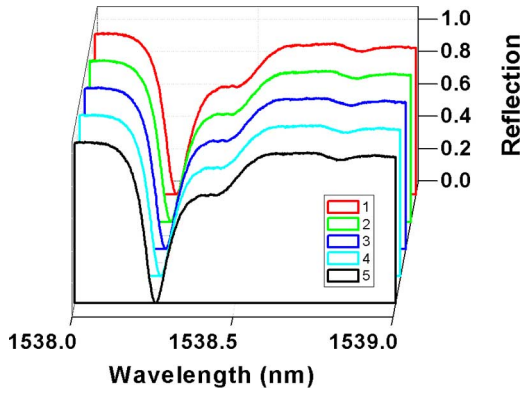

Fig. 10. The stability of the PZT-induced notch filter.

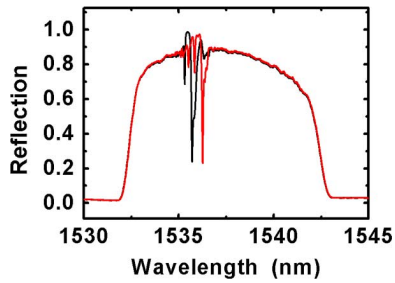

Fig. 11. The wavelength tunability of the PZT-induced phase shift when the voltage is applied on the two PZTs in turn.

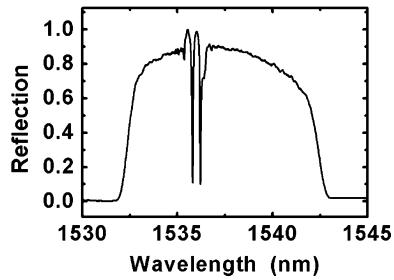

Fig. 12. The measured reflection when two PZTs are simultaneously utilized to generate two notches.

Secondly, another chirped FBG with two glued PZTs is utilized to investigate the tunability of the resulted notch filter. This FBG has roughly the same characteristic as the last one, i.e., the grating strength, bandwidth, and length are also 10 dB, 10 nm, and 12 cm, respectively. The position gap between the two PZTs on the grating is 0.6 cm. Fig. 11 shows reflection spectrum obtained when the voltage is applied on the two PZTs in turn. Note that, due to the fabrication issue, the spectrum of the original grating is uneven here. Nonetheless, it can be seen that the notch wavelength has been shifted by a step of 0.482 nm, which agrees well with the simulation result shown in Fig. 4. Fig. 12 shows the spectrum for the dual notch filters while the voltages 120 V and 140 V are simultaneously applied on the two PZTs, respectively. The wavelength separation between the dual notches measured is about 0.492 nm, coinciding with the results shown in Fig. 5.

Here it must be pointed that the working voltage applied to the PZT is about 150 V, higher than those ones reported in the

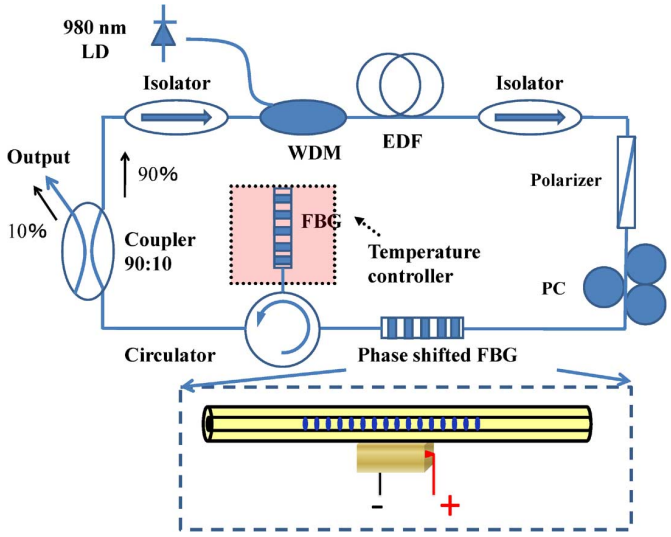

Fig. 13. Experimental setup for the SLM EDF ring laser, where the inset illustrates the schematic diagram of the phase shift induced by PZT as shown in Fig. 1.

previous papers [22]. We believe that the voltage can be significantly reduced if a more suitable PZT is selected.

E. Application of the Phase-Shifted FBG to a Fiber Laser

Next, by utilizing the phase shifted FBG described above, an EDF-based fiber ring laser capable of working with SLM is demonstrated. Fig. 13 shows the schematic diagram of the experimental setup, where a 980 nm pumping source, 5-m-length EDF (enabling to provide a maximum gain of about 14 dB at 1550 nm), two isolators for unidirectional optical propagation, one polarizer and one polarization controller (PC) used both for eliminating the birefringence induced notch splitting and for stabilization of the laser output, one 10/90 power coupler, one circulator, a temperature controller and two concatenated linearly-chirped FBGs are included. Inset of the Fig. 13 shows the schematic diagram for the phase shifts induced by the PZTs as shown in Fig. 1. An ultra-narrow bandpass filter can be formed by utilizing the two gratings which have identical characteristics but one of them (without the glued PZT) working in the reflection is placed in a temperature chamber which can be used to shift the spectrum a little by controlling the temperature and the other (with the phase-shift induced by PZT) is working in the transmission [3]. Fig. 14 shows the measured transmission spectrum while the voltage applied on the PZT is 150 V. It can be seen that a bandpass filter with a center wavelength of 1538.21 nm, 3-dB bandwidth of ∼0.088 nm, a height of 7.5 dB is successfully obtained. The two sidelobes existed near the both ends of the original FBG's spectrum are due to the overlap between the transmission and the reflection spectrum of the two FBGs with nonideal rising and falling edges. The difference between the main peak and the sidelobes is larger than 6 dB, which is large enough to guarantee the laser lasing at the main peak wavelength. Moreover, the whole length of the fiber ring is about 35 m (producing a mode spacing of ∼5.8 MHz) and the total loss is estimated to be 11 dB. Fig. 15 shows the measurement results for the lasing spectrum, while the 980 nm-LD pump power is 74 mW. The maximum output power is −27 dBm. The laser

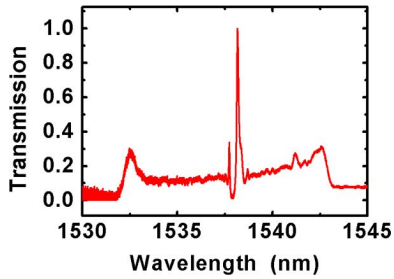

Fig. 14. Spectrum of the narrow bandpass filter formed by incorporating the transmission and reflection spectrum of the two FBGs, respectively.

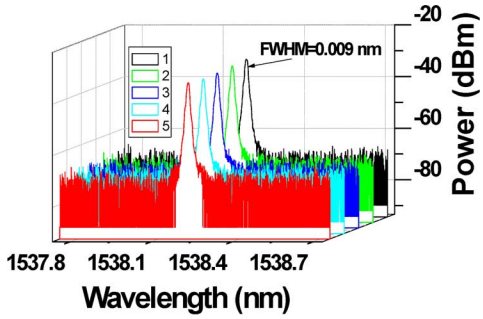

Fig. 15. Output spectra of the fiber ring laser measured in every five minutes.

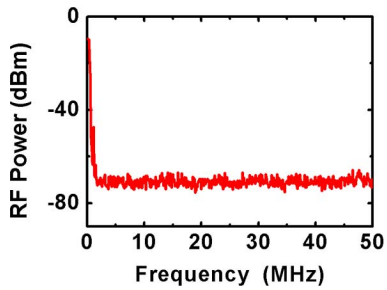

Fig. 16. RF spectrum of the output laser when the EDF is used as a gain medium.

linewidth is about 0.009 nm measured by the OSA with a limited resolution of 0.01 nm. The peak wavelength of the laser is 1538.21 nm, which agrees well with the filter shown in Fig. 14. Stability for the produced laser lasing is also investigated. Five measurements of the reflection spectrum performed every other five minute are also shown in Fig. 15 and no change for the lasing power and the peak wavelength can be found during the five measurements. Fig. 16 shows the RF spectrum of the laser output. It is seen that the RF spectrum is in the range of 0 to 50 MHz, which is wide enough to capture the beat signals. No beat signal has been found, which in return indicates that the SLM operation status is confirmed in this fiber laser.

III. Conclusion

In conclusion, temporary phase shifts induced by the mini-size PZTs in a FBG are demonstrated. The induced phase-shift can be controlled by changing the voltage applied on the PZT and the induced notch is both stable and switchable. Based on the PZT-induced phase-shifted FBG, a single-longitudinal-mode Erbium doped fiber ring laser has been successfully demonstrated. This kind of phase-shifted FBG is expected to

find the potential applications on multiwavelength fiber lasers by inserting either one phase shift in a sampled FBG or multiple phase shifts simultaneously in a one-channel FBG.

REFERENCES

[1] W. Loh and R. Laming, "1.55 μm phase-shifted distributed feedback fibre laser," *Electron. Lett.*, vol. 31, no. 17, pp. 1440–1442, 1995.

[2] A. Asseh, H. Storoy, J. Kringlebotn, W. Margulis, B. Sahlgren, S. Sandgren, R. Stubbe, and G. Edwall, "10 cm Yb^{3+} DFB fibre laser with permanent phase shifted grating," *Electron. Lett.*, vol. 31, no. 12, pp. 969–970, 1995.

[3] M. Li, X. Chen, T. Fujii, Y. Kudo, H. Li, and Y. Painchaud, "Multiwavelength fiber laser based on the utilization of a phase-shifted phase-only sampled fiber Bragg grating," *Opt. Lett.*, vol. 34, no. 11, pp. 1717–1719, 2009.

[4] G. Agrawal and S. Radic, "Phase-shifted fiber Bragg gratings and their application for wavelength demultiplexing," *IEEE Photon. Technol. Lett.*, vol. 6, no. 8, pp. 995–997, 1994.

[5] D. Gatti, G. Galzerano, D. Janner, S. Longhi, and P. Laporta, "Fiber strain sensor based on a π-phase-shifted Bragg grating and the pound-drever-hall technique," *Opt. Exp.*, vol. 16, no. 3, pp. 1945–1950, 2008.

[6] A. Iadicicco, A. Cusano, A. Cutolo, R. Bernini, and M. Giordano, "Thinned fiber Bragg gratings as high sensitivity refractive index sensor," *IEEE Photon. TechnOL. Lett.*, vol. 16, no. 4, pp. 1149–1151, 2004.

[7] N. Berger, B. Levit, B. Fischer, M. Kulishov, D. Plant, and J. Azaña, "Temporal differentiation of optical signals using a phase-shifted fiber Bragg grating," *Opt. Exp.*, vol. 15, no. 2, pp. 371–381, 2007.

[8] M. Asghari and J. Azaña, "Design of all-optical high-order temporal integrators based on multiple-phase-shifted Bragg gratings," *Opt. Exp.*, vol. 16, no. 15, pp. 11 459–11 469, 2008.

[9] R. Kashyap, P. Mckee, and D. Armes, "UV written reflection grating structures in photosensitive opticalfibres using phase-shifted phase masks," *Electron. Lett.*, vol. 30, no. 23, pp. 1977–1978, 1994.

[10] D. Anderson, V. Mizrahi, T. Erdogan, and A. White, "Production of in-fibre gratings using a diffractive optical element," *Electron. Lett.*, vol. 29, no. 6, pp. 566–568, 1993.

[11] J. Canning and M. Sceats, "π-phase-shifted periodic distributed structures in opticalfibres by UV post-processing,," *Electron. Lett.*, vol. 30, no. 16, pp. 1344–1345, 1994.

[12] I. D. Villar, F. Arregui, I. Matias, A. Cusano, D. Paladino, and A. Cutolo, "Fringe generation with non-uniformly coated long-period fiber gratings," *Opt. Exp.*, vol. 15, no. 15, pp. 9326–9340, 2007.

[13] A. Iadicicco, S. Campopiano, A. Cutolo, M. Giordano, and A. Cusano, "Microstructured fibre Bragg gratings: Analysis and fabrication," *Electron. Lett.*, vol. 41, no. 8, pp. 466–468, 2005.

[14] A. Cusano, D. Paladino, and A. Iadicicco, "Microstructured fiber Bragg gratings," *J. Lightw. Technol.*, vol. 27, no. 11, pp. 1663–1697, May 2009.

[15] J. Kringlebotn, J. Archambault, L. Reekie, and D. Payne, "$Er^{3+}:Yb^{3+}$ -codoped fiber distributed-feedback laser," *Opt. Lett.*, vol. 19, no. 24, pp. 2101–2103, 1994.

[16] M. Janos and J. Canning, "Permanent and transient resonances thermally induced in optical fibre Bragg gratings," *Electron. Lett.*, vol. 31, no. 12, pp. 1007–1009, 1995.

[17] D. Uttamchandani and A. Othonos, "Phase shifted Bragg gratings formed in optical fibres by post-fabrication thermal processing," *Opt. Commun.*, vol. 127, no. 4–6, pp. 200–204, 1996.

[18] S. Li, N. Ngo, S. Tjin, P. Shum, and J. Zhang, "Thermally tunable narrow-bandpass filter based on a linearly chirped fiber Bragg grating," *Opt. Lett.*, vol. 29, no. 1, pp. 29–31, 2004.

[19] M. Li, H. Li, and Y. Painchaud, "Multi-channel notch filter based on a phase-shift phase-only sampled fiber Bragg grating," *Opt. Exp.*, vol. 16, no. 23, pp. 19388–19394, 2008.

[20] A. Ahuja, P. Steinvurzel, B. Eggleton, and J. Rogers, "Tunable single phase-shifted and superstructure gratings using microfabricated on-fiber thin film heaters," *Opt. Commun.*, vol. 184, no. 1–4, pp. 119–125, 2000.

[21] Z. Zhang, C. Tian, M. Roelens, M. Mokhtar, P. Petropoulos, D. Richardson, and M. Ibsen, "Direct characterization of the spatial effective refractive index profile in Bragg gratings," *IEEE Photon. Technol. Lett.*, vol. 17, no. 12, pp. 2685–2687, Jun. 2005.

[22] M. Xu, A. Alavie, R. Maaskant, and M. Ohn, "Tunable fibre bandpass filter based on a linearly chirped fibre Bragg grating for wavelength demultiplexing," *Electron. Lett.*, vol. 32, no. 20, pp. 1918–1919, 1996.

[23] I. Jauncey, L. Reekie, J. Townsend, C. Rowe, and D. Payne, "Single-longitudinal-mode operation of an Nd^{3+} -dopedfibre laser," *Electron. Lett.*, vol. 24, no. 1, pp. 24–26, 1988.

[24] G. Ball and W. Morey, "Continuously tunable single-mode erbium fiber laser," *Opt. Lett.*, vol. 17, no. 6, pp. 420–422, 1992.

[25] M. Guy, J. Taylor, and R. Kashyap, "Single-frequency erbium fibre ring laser with intracavityphase-shifted fibre Bragg grating narrowband filter," *Electron. Lett.*, vol. 31, no. 22, pp. 1924–1925, 1995.

[26] X. Cheng, P. Shum, C. Tse, J. Zhou, M. Tang, W. Tan, R. Wu, and J. Zhang, "Single-longitudinal-mode erbium-doped fiber ring laser based on high finesse fiber Bragg grating fabry-perot etalon," *IEEE Photon. Technol. Lett*, vol. 20, no. 12, pp. 976–978, 2008.

[27] A. Suzuki, Y. Takahashi, M. Yoshida, and M. Nakazawa, "An ultralow noise and narrow linewidth $\lambda/4$-shifted DFB ER-doped fiber laser with a ring cavity configuration," *IEEE Photon. Technol. Lett.*, vol. 19, no. 19, pp. 1463–1465, 2007.

[28] H. Quynhanh, A. Suzuki, M. Yoshida, T. Hirooka, and M. Nakazawa, "A $\lambda/4$-Shifted distributed-feedback laser diode with a fiber ring cavity configuration having an OSNR of 85 dB and a linewidth of 7 kHz," *IEEE Photon. Technol. Lett.*, vol. 20, no. 18, pp. 1578–1580, Sep. 2008.

[29] G. Ball, W. Morey, and W. Glenn, "Standing-wave monomode erbium fiber laser," *IEEE Photon. Technol. Lett.*, vol. 3, no. 7, pp. 613–615, Jul. 1991.

[30] M. Li, T. Fujii, and H. Li, "Multiplication of a multichannel notch filter based on a phase-shifted phase-only sampled fiber Bragg grating," *IEEE Photon. Technol. Lett.*, vol. 21, no. 13, pp. 926–928, Nov. 2009.

[31] T. Erdogan, "Fiber grating spectra," *J. Lightw. Technol.*, vol. 15, no. 8, pp. 1277–1294, 1997.

[32] J. Skaar, L. Wang, and T. Erdogan, "On the synthesis of fiber Bragg gratings by layer peeling," *IEEE J. Quantum Electron.*, vol. 37, no. 2, pp. 165–173, 2001.

[33] H. Li, M. Li, Y. Sheng, and J. E. Rothenberg, "Advances in the design and fabrication of high-channel-count fiber Bragg gratings," *J. Lightw. Technol.*, vol. 25, no. 9, pp. 2739–2750, Sep. 2007.

[34] H. Li, T. Kumagai, and K. Ogusu, "Advanced design of a multichannel fiber Bragg grating based on a layer-peeling method," *J. Opt. Soc. Amer. B*, vol. 21, no. 11, pp. 1929–1938, 2004.

Xuxing Chen received the B.Sc. and M.S. degrees from Nanjing Normal University, China, in 2004 and 2007, respectively. Currently, he is pursuing the Ph.D. degree at Shizuoka University, Hamamatsu, Japan.

His research interests involve nonlinear fiber optics, fiber lasers and fiber Bragg gratings.

Yves Painchaud, photograph and biography unavailable at time of publication.

Kazuhiko Ogusu, photograph and biography unavailable at time of publication.

Hongpu Li (M'00) received the B.S. and M.S. degrees from Huazhong University of science and technology, Wuhan, China, in 1985 and 1988, respectively, and received the Ph.D. degree from Shizuoka University, Hamamatsu, Japan in 2000.

From 1988 to 1996, he had been worked at the State Key Laboratory of Laser Technology, Huazhong University of Science and Technology, China. From 2000 to 2003, first, he was with the NEC Research Institute, NJ, then the Phaethon Communication Inc., CA, and then the Laval University, Canada. In April 2003, he joined to the Shizuoka University, Japan. Now he is an associate professor at the Department of Electrical and Electronic Engineering. His current research interests include the nonlinear fiber optics, microwave photonics, fiber lasers, fiber gratings, all-optical switching, and optical information processing etc. He has authored more than 100 refereed journal and conference papers and held several U.S. patents.

Dr. Li is a member of OSA and IEEE Photonics Society.